NH_3 on the MgO{100} surface: the concentration dependence of tunnelling spectra

1997 J. Phys.: Condens. Matter 9 43

(http://iopscience.iop.org/0953-8984/9/1/007)

J. Phys.: Condens. Matter **9** (1997) 43–52. Printed in the UK PII: S0953-8984(97)76165-4

NH_3 on the MgO{100} surface: the concentration dependence of tunnelling spectra

M Prager†, M Havighorst†, G Coddens‡ and H Büttner§

† Institut für Festkörperforschung der KFA Jülich, D-52425 Jülich, Germany
‡ Laboratoire Leon Brillouin, CEA Saclay, F-91191 Gif-sur-Yvette, France
§ Institut Laue–Langevin, F-38042 Grenoble Cédex, France

Received 10 July 1996, in final form 23 October 1996

Abstract. Ammonia adsorbed on a MgO{100} surface represents a model system of a molecule in an environment of incompatible symmetry. High-resolution neutron spectroscopy was used to measure the rotational spectra of ammonia molecules at nine different coverages in the range 0.01 ML $\leqslant \theta \leqslant$ 0.89 ML. The energies of the four lowest rotational levels are derived and analysed within the rotation–translation-coupling model. The situation with isolated molecules is realized at very low concentrations. With increasing coverage, intermolecular interaction leads to an increase of the strength of the rotational potentials, but ammonia molecules do not order orientationally below $\theta \sim 0.62$ ML. The centre-of-mass eccentricity stays constant. At the highest coverages $\theta \geqslant 0.62$ ML, intermolecular interaction dominates and suppresses tunnelling. A model of coexisting phases is presented to explain simultaneously the sharpness of the tunnelling lines and the variation of their energy and intensity with coverage.

1. Introduction

Rotational tunnelling spectroscopy is used as an especially sensitive method to determine rotational potentials of small molecules or molecular sidegroups and therefrom the intermolecular interactions. The pronounced sensitivity is based on the exponential decrease of the overlap of the molecular wave functions of librational states with increasing barrier height. This property yields also a very strong dependence on the symmetry of the rotational potential. A potential of higher multiplicity has narrower barriers and allows a larger overlap which is related to significantly larger splittings.

Neutron tunnelling spectroscopy so far has been mainly used to study bulk materials. Only few surface systems have been investigated. The main restriction consists in the large specific surface area required to get a measurable signal. This condition is fulfilled by the basal planes of graphite and appropriately prepared magnesium oxide MgO with {100} surfaces. Three-dimensional rotation is most readily investigated in the case of the nonpolar spherical top methane adsorbed on Grafoil. The effect of site symmetry could be shown and the strength of the rotational potential was derived from atom–atom potentials [1, 2]. Methane was similarly studied when adsorbed on MgO [3]. Ammonia differs from methane in two ways. First, it is a one-dimensional rotor experiencing—secondly—strong electrostatic interaction due to a dipole moment of $1.47D$. This interaction leads to 3d ammonia aggregates on nonpolar graphite surfaces. On a polar MgO surface, however, the NH_3 molecules do not cluster, and they show, at low coverage, almost free quantum rotation [4].

0953-8984/97/010043+10$19.50

The concept used most generally to interpret rotational tunnelling spectra is the single-particle (SP) model [5] which assumes the molecule to have a fixed centre of mass and not to couple orientationally to other molecules. The interactions with the lattice atoms are globally contained in a—at low temperature static—rotational potential. This concept with its simple relation between rotational excitations and potential parameters is very successful in describing spectroscopic results for a wide range of barrier heights and for many materials [6].

Recently systems have been found whose spectra cannot be interpreted consistently within the SP model: the description requires unusually strong intermolecular interactions. This failure is taken as an indication of more complex dynamics. In two cases, the Hofmann clathrates [7, 8] and ammonia adsorbed at the {100} surfaces of MgO at a coverage $\theta = 0.1$ ML [4], a potential surface which classically would invoke a coherent reverse rotation of the molecule and its centre of mass (c.o.m.) has been found to describe the observed features uniquely well. The Hamiltonian of such a coupled motion is [9, 10]

$$H = -B_{\mathrm{NH_3}}\frac{\partial^2}{\partial\varphi^2} - B_{c.o.m.}\left(\frac{\partial}{\partial\alpha} - \frac{\partial}{\partial\varphi}\right)^2 + 2A_1\cos(3\varphi + 4\alpha) + 2A_2\cos(4\alpha). \tag{1}$$

$B_{\mathrm{NH_3}}$ and $B_{c.o.m.}$ represent the respective rotational constants, α is the angle of rotation of the centre of mass with eccentricity R in the crystal frame, and φ is the angle of rotation of the ammonia group with respect to the rotating c.o.m. frame. The potential surface of this so-called rotation–translation-coupling (RTC) model is characterized by the two parameters A_1 and A_2. They are the only free parameters of the model. The eccentricity R and therewith the rotational constant $B_{c.o.m.}$ are determined by the potential parameters via the relations

$$R = \rho\sqrt[3]{\frac{4A_2}{A_1}} \qquad B_{c.o.m.} = \frac{\hbar^2}{2m_{tot}R^2}. \tag{2}$$

m_{tot} is the total mass of the rotor. A_1 describes the rotational potential of the ammonia molecule for any fixed offset position (α, R) of the c.o.m., while A_2 is the potential along a path $3\varphi + 4\alpha =$ constant in parameter space.

In classical mechanics the potential surface favours a correlated internal rotation and c.o.m. motion, which indeed was observed for other systems by diffraction [9]. For our system, classical first-principles calculations [11] show that the ammonia adsorbs at an off-centre position with one hydrogen atom oriented towards one oxygen atom of the substrate. At high temperature, thermal motion makes this in-plane orientation fluctuate stochastically between all four nearest oxygen atoms of the substrate. When the temperature is of the order of the barrier height for internal rotation, the two rotations become coupled in the way described by the RTC model.

In the present work we want to study whether—and, if so, how—increasing intermolecular interaction due to increasing coverage of the surfaces modifies the RTC dynamics.

2. Experimental procedure and results

Commercially available MgO powder (Merck GmbH) was used. The sample preparation followed the procedure outlined in a previous publication [4]. Pellets of the material of about 3 g each were prepared at a pressure of 150 bar. They were cleaned and outgassed in a vacuum at $T = 900\ ^\circ$C for 20 h. Ten pellets with an integral weight of 30 g MgO were transferred under Ar atmosphere into a 0.2 mm thin-walled steel container and outgassed

again at $T = 600$ °C for 2 h. The final vacuum at the sample was $\sim 1 \times 10^{-6}$ mbar. After such treatment, {100} surfaces dominate and the samples show a specific surface area of 57 $m^2\ g^{-1}$ as determined from krypton adsorption isotherms [12] taken at $T = 77.3$ K. NH_3 adsorption isotherms taken at $T = 192$ K are of BET type-II shape (figure 1) and show clearly that the NH_3 does not form three-dimensional clusters, but wets the surface. An appropriate analysis of the data [13] yields the amount of material required for monolayer (ML) completion, $\theta' = 1$ ML, together with a specific area per molecule of 11.2 $Å^2$. This value is consistent with an incommensurate dense hexagonal packing of ammonia molecules. Nominal coverages θ' based on the interpretation of isotherms were chosen in the range 0.12 ML $\leqslant \theta' \leqslant$ 0.91 ML NH_3. The true {100} coverage is called θ. It is outlined below how θ is obtained from the measurements. All further discussions refer to the true coverage θ.

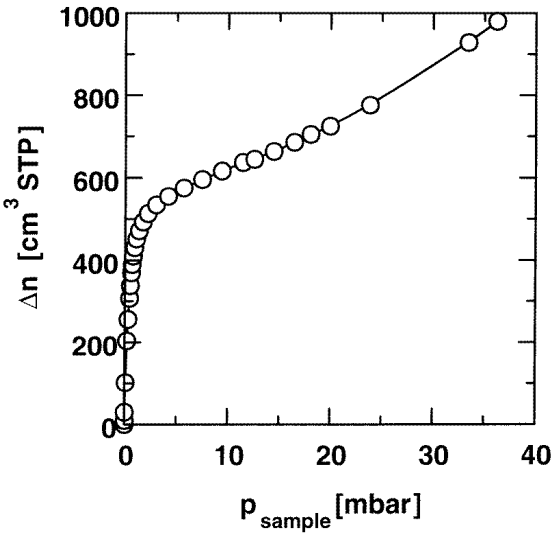

Figure 1. The adsorption isotherm of NH_3 on MgO{100} taken at a substrate temperature of $T = 192$ K.

Inelastic neutron scattering spectra were obtained with two spectrometers. First, the time-of-flight spectrometer MIBEMOL at LLB, Saclay, France, was used at various wavelengths 3 Å $\leqslant \lambda \leqslant$ 8 Å related to energy resolutions 300 μeV $\geqslant \delta E \geqslant$ 50 μeV. These measurements were completed to a denser grid of coverages using the time-of-flight spectrometer IN5 at ILL, Grenoble, France, at similar wavelengths. Spectra were generally taken at sample temperatures $T = 5$ K. As an example, figure 2 shows the sum over all detectors in the range of scattering angles $50° \leqslant 2\vartheta \leqslant 140°$, and corrected for background for a coverage $\theta = 0.24$ ML. A number of Gaussians were combined into a scattering function for a quantitative description of the data. This theoretical function was convoluted with the measured instrumental resolution. The fit is shown as a solid line. The positions of the observed inelastic transitions at all coverages including those from earlier work [4] are reported in the upper part of table 1.

It was checked that commercially available MgO powder obtained by dehydration of magnesium hydroxide shows the same behaviour as the powders used in the literature, which were made by burning metallic Mg in a mixed krypton–oxygen atmosphere [12]. Those

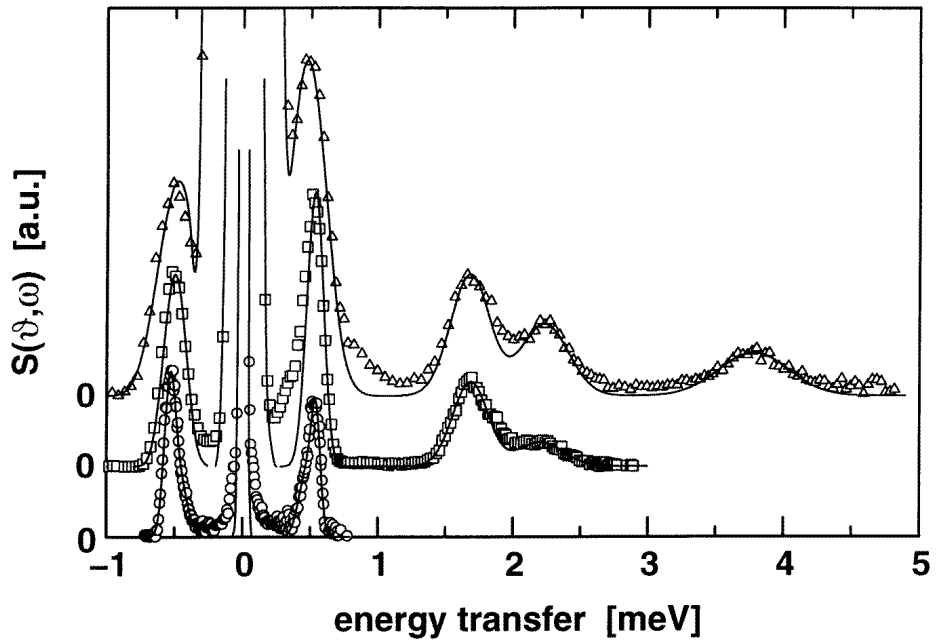

Figure 2. Tunnelling spectra of 0.24 ML NH_3 on MgO{100}. Spectrometer: IN5, ILL, Grenoble. $\lambda = 7.8, 4.5$ and 3.7 Å with resolutions $\delta E = 30, 110$ and 270 μeV. The sample temperature $T_S = 5$ K. Solid lines show the fit, symbols the observed spectra.

powders are called 'standard' in the following. At first the adsorption isotherms from the Merck powder are very similar to those obtained from the standard. Electron micrographs of the standard powder show nice MgO cubes with near-to-ideal {100} surfaces. Secondly, neutron spectra taken at identical coverages from the commercial and the standard powder were almost identical. The statistics of the data from the Merck powder, however, is significantly better due to the much larger specific surface.

The intensity of the fundamental tunnelling transition changes characteristically with coverage. It is expected that the intensity of the tunnelling lines will increase linearly with the coverage of the {100} surface if additional molecules are adsorbed on identical sites. For the samples of low nominal coverage θ' this is the case only *above a threshold value* $\theta'_0 = 0.105$. Such a behaviour is attributed to the imperfection of the substrate. Adsorbed molecules first saturate these sites with their stronger binding energies before {100} planes are occupied. Calculations for very small crystallites have shown that edges are indeed favoured adsorption sites [14]. If we call the coverage of the completed hcp monolayer $\theta_1 = 1.0$, then the true coverage of the {100} surface is obtained from the nominal one via the relation

$$\theta = \frac{\theta' - \theta'_0}{1 - \theta'_0}. \tag{3}$$

For each coverage all observed transitions can be assigned to *one* level scheme according to table 1. The levels are labelled by numbers, starting with 0 for the ground state. For comparison the levels of the free one-dimensional NH_3 rotor FR are included. The changes with coverage are more clearly displayed in a graphic presentation (figure 3). Spectra were

Table 1. Upper part: observed rotational transitions in meV of NH_3 on MgO{100} surfaces at various coverages θ. Samples temperature: $T_S = 5$ K. No tunnelling is observed at coverages $\theta \geqslant 0.7$ ML. FR refers to the case of the free rotor. Lower part: potential parameters of the RTC model [10] (equation (1)), eccentricities R (equation (2)) and rotor levels calculated for these parameters.

θ (ML)	0.012	0.065	0.105	0.16	0.24	0.38	0.56	0.66	FR
Transition									
0→1	0.610	0.610	0.618	0.598	0.540	0.484	0.470	0.44	0.782
0→1			0.599	0.540	0.470	0.442	0.408		
1→2		1.76	1.76	1.72	1.68	1.56	1.67		2.35
0→2		2.37	2.37	2.30	2.20	1.99	2.06		3.13
1→3			4.10	3.92	3.76	3.52			6.26
0→3			4.74	4.56	4.30	4.08			7.04
Potential									
A_1 (meV)			4.58	4.00	8.48	14.6			
A_2 (μeV)			2.58	2.78	3.78	7.76			
R (Å)			0.123	0.132	0.114	0.121			
Calculated levels (meV)									
1			0.611	0.610	0.533	0.446			
2			2.33	2.30	2.08	1.77			
3			4.79	4.56	4.49	3.93			

measured up to a temperature $T = 70$ K for $\theta = 0.105$ ML. The evolution of the ratio of up and down scattering line intensities fully supports the proposed assignment.

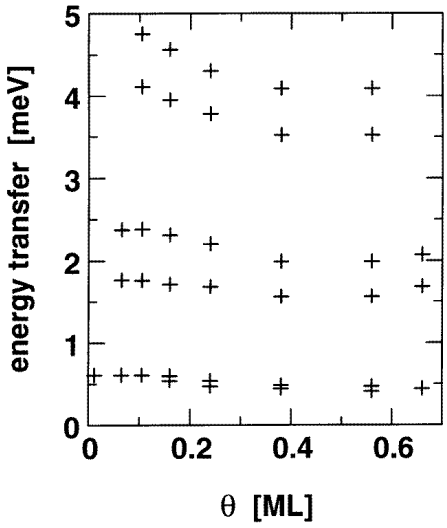

Figure 3. Dependences of the rotational transition energies of NH_3 adsorbed on MgO on the coverage θ of the {100} surfaces. Sample temperature: $T_S = 5$ K.

Intensities were not measured on an absolute scale. Due to the identical sample volumes the intensities of the transitions from different samples measured in one set-up of a given

spectrometer can be compared to each other, however. When comparing data from the two different spectrometers used, *one* arbitrary factor has to be introduced. This factor is based on results from identical samples ($\theta \sim 0.10$ ML) for which measurements were made with both instruments. For reasons of intensity, IN5 was used for samples of low coverages with shorter wavelength. The line intensities of such data sets were transformed to the standard configuration by correcting for monitor efficiency ($\sim 1/v$) and change of inelastic structure factor with momentum transfer. With these corrections the intensity of the fundamental tunnelling transition with increasing coverage is shown in figure 4. The zero-point long-dashed line shows the increase of (normalized) intensity at low coverages. The opposite behaviour, a linear *reduction* of intensity, is found at intermediate coverages. The various lines in the figure are discussed below.

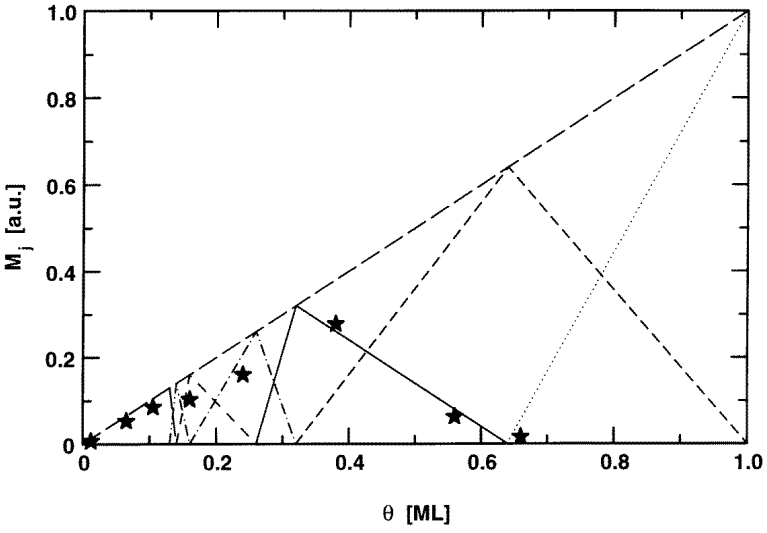

Figure 4. The intensity of the fundamental tunnelling transition of NH_3 as a function of coverage θ of the MgO{100} surfaces. The various lines describe the growth and disappearance of different surface structures in the model of coexisting phases (section 3.2). Sample temperature: $T_S = 5$ K.

3. Discussion

The interpretation of the outlined results requires the knowledge of the adsorption geometry. Diffraction experiments do not yet exist. Thus energy-minimization calculations for low coverages are used as alternative sources of information. They show the electrostatic interaction dominating over all other forces, and the ammonia being bound at a distance from the surface of 2.5 Å via the N to a Mg atom with the molecular symmetry axis perpendicular to the surface [15–17]. A recent *ab initio* calculation [11] yields additionally an inclination of the molecule. IR spectra are successfully interpreted on the basis of this adsorption geometry [18]. The (almost) parallel ammonia molecules represent repulsive dipoles and are expected to cover the surface homogeneously. These conclusions are in agreement with the observation of BET type-II adsorption isotherms characteristic of monolayer formation.

3.1. Model-independent analysis of the spectra

The most remarkable feature of the tunnelling spectra is the existence of two regimes of coverage-independent transition energies but linearly varying intensities.

At coverages $\theta \leqslant 0.10$ ML the transition energies are constant, $\hbar\omega_{0\to1} = 0.610$ meV, and the transition intensities *increase* proportionally to θ. If the molecules are distributed homogeneously on the {100} surfaces according to the dipolar repulsion, then the intermolecular nearest-neighbour distances are $d_{\mathrm{MM}} \geqslant 10$ Å in this regime. This is much larger than the distance of the NH_3 from the surface. Thus the potential surface is dominated by the interaction with the substrate and we observe the situation of *isolated molecules*. Compared to the free-rotor energy $\hbar\omega_{FR} = 0.782$ meV the $0 \to 1$ transition is significantly reduced by a finite rotational potential. The linear increase of the intensity is the natural consequence of the increasing number of molecules at identical adsorption sites.

In a broad intermediate-concentration range 0.30 ML $\lesssim \theta \lesssim$ 0.65 ML a situation is observed where the tunnelling splitting again remains constant (figure 3). It is significantly reduced, $\hbar\omega_{0\to1} \sim 0.47$ meV, compared to the case of the isolated molecule with $\hbar\omega_{0\to1} = 0.610$ meV. Thus intermolecular interaction must contribute a significant part to the rotational potential. The sharpness of the tunnelling transitions—especially those to higher levels which show larger absolute shifts with increasing potential strengths—is again consistent with the presence of *unique adsorption sites*. In this second regime the intensity of the fundamental tunnelling transition *decreases with coverage*. A straight line connecting the points in this concentration regime intersects the abscissa at a characteristic coverage $\theta_I \sim 0.62$ ML and the zero-point long-dashed straight line at $\theta_{II} \sim 0.31$ ML $= \theta_I/2$ (figure 4). A point on this line is characterized by crystallographically identical molecules. Beginning with coverage θ_{II}, tunnelling sites are lost with further adsorption until almost none are left at $\sim\theta_I$. The lost inelastic intensity reappears as elastic scattering and the total scattering increases proportionally to the total number of ammonia molecules adsorbed.

In the 0.1 ML $\leqslant \theta \leqslant$ 0.31 ML region two coverages were studied. The reduction of the tunnelling splitting compared to that of the isolated molecule indicates the onset of interaction between adsorbed molecules. Within experimental accuracy the intensities of the tunnelling transitions continue to increase almost proportionally to coverage, as already found for the very low concentrations. The weak underestimation of the tunnelling intensity is to a great extent a consequence of the better energy resolution of the IN5 instrument: some of the inelastic intensity between the elastic and tunnelling line is now not contained in the Gaussian line modelling the transition. Again the tunnelling transitions are reasonably sharp, as expected for well defined adsorption sites.

For $\theta \geqslant 0.7$ ML no tunnelling transitions are observed. In this regime the molecules in the adsorbed layer become rather densely packed with c.o.m. distances below 4.2 Å (table 2). Such intermolecular spacings are close to that of solid pure ammonia [19]. Taking into account an N–H bond length of 1.04 Å, the protons of neighbouring molecules might approach each other up to almost 2 Å. The coupling of such coplanar molecules is especially pronounced and related to a strong barrier to rotation with unresolvable tunnel splitting.

3.2. The model of coexisting commensurate phases

The existence of broad regimes of coverages with constant tunnel splitting requires not only a fixed adsorption site but also a coverage-independent stable molecular environment. At the same time the smooth evolution of line intensities requires a gradual build-up or destruction

of areas of the respective structures. Under the restriction that the ammonia molecule is bound to a Mg atom of the surface these two conditions are simultaneously fulfilled for *coexisting commensurate phases* of neighbouring density. Pure phases are related to characteristic concentrations. Table 2 shows all squaric structures characterized by the lattice vectors of the surface unit cell in units of the Mg–Mg distance $d_{\mathrm{MgMg}} = 2.98$ Å, the related characteristic concentration, and the related centre-of-mass distances of nearest molecular neighbours down to $\theta = 0.10$ ML. The characteristic coverages θ_I and θ_{II} extracted from the spectra are found in this table. At an arbitrarily chosen coverage, tunnelling lines characteristic of the next-closest phases appear in the spectrum with intensities proportional to the number of molecules in the corresponding phases. This variation is shown by the various dashed lines in figure 4. On the basis of this model, NH_3 in both the dense hcp (the dotted line) and the $\sqrt{2} \times \sqrt{2}$ (the short-dashed line) phases does not show tunnelling. The tunnelling transition at $\hbar\omega = 0.44$ meV appears as a fingerprint of the 2×2 phase (the solid line) at $\theta_I \sim 0.64$ ML when the concentration is just too low to complete the $\sqrt{2} \times \sqrt{2}$ structure. At $\theta_{II} = 0.32$ ML *all* molecules will have moved into this phase, thus yielding the spectrum with the most intense tunnelling lines. (A similar model was used earlier to explain the variation of tunnelling spectra of ammonia adsorbed into caesium in stage-2 caesium-intercalated graphite as a function of the amount of intercalated ammonia [21].)

Table 2. Coverages θ_i for which pure squaric phases with next-neighbour distances d_{MM} of ammonia molecules are realized.

i	θ_i (ML)	Unit cell (d_{MgMg})	d_{MM} (Å)
hcp	1.0	Incommensurate	3.60
I	0.64	$\sqrt{2} \times \sqrt{2}$	4.21
II	0.32	2×2	5.96
III	0.26	$\sqrt{5} \times \sqrt{5}$	6.66
IV	0.16	$\sqrt{8} \times \sqrt{8}$	8.43
V	0.14	3×3	8.94
VI	0.13	$\sqrt{10} \times \sqrt{10}$	9.42
VII	0.10	$\sqrt{13} \times \sqrt{13}$	10.74

With further decreasing concentration, the stability range of subsequent phases narrows more and more. In agreement with the outlined model some spectra can be fitted as a superposition of two spectra of coexisting phases (table 1). Finally, at low concentrations ordered phases will no longer be formed since the driving force for the phase transitions, the repulsive intermolecular interaction, becomes too small. Here the simpler model of an adsorbed isolated molecule [4] can be used.

Diffraction experiments are needed to confirm—or may lead to modifications of—the details of the outlined structural model.

3.3. Rotation–translation-coupling and beyond

At low coverages only the RTC model [9, 10] yielded a description consistent with atom–atom potentials [4]. The smooth evolution of spectra with coverage shows that RTC is characteristic for the denser phases too. Potential parameters deduced from equation (1) and the corresponding calculated rotational levels are presented in the lower part of table 1. Both terms of the potential increase systematically with increasing coverage due to the increasing contribution of the interaction between the adsorbed molecules. At the same time

their ratio A_2/A_1 varies little. This ratio determines the eccentricity R of the c.o.m. motion which stays almost constant at all coverages (table 1). Globally, the RTC model describes the experimental spectra (table 1, upper part) less well at higher coverages.

Based on the structural model derived, a calculation of potential surfaces from atom–atom potentials can be extended to denser adsorbates by including interaction between NH_3 molecules. For the dominant Coulomb interaction the charges of the ammonia molecules in the adsorbate are modelled by the squaric proton density distribution $\rho = \Psi \cdot \Psi^*$. A central molecule of 'classical' triangular shape explores the corresponding potential surface in (α, φ)-space. The off-centre geometry of the adsorption site is reproduced by such calculations.

The RTC approach models the NH_3 c.o.m. motion as pure translation and neglects the weak inclination of the Mg–N bond axis found in *ab initio* calculations [11]. Such an inclination reduces the dipolar energy and thus looks intuitively reasonable. For the same reason the molecules in pure ammonia form a complex orientational spin pattern [19] with four sublattices. Thus the characteristic coupled motion is in reality a nutation of the whole molecule and the internal rotation. It is very probably present in many materials where a chemical bond restricts molecular motion to the surface of a sphere. The corresponding Hamiltonian should be studied. However, despite its simplicity, the RTC model works well even for large coverages.

The dipolar coupling might also lead to collective in-plane tunnelling. The underlying theory is still not fully solved for a linear chain [20], however.

4. Conclusion

Molecular adsorbates can represent exciting tunnelling systems, since such fundamental parameters as the intermolecular interaction can be influenced easily by simply varying the density of the adlayer.

Ammonia molecules adsorbed at all coverages $\theta \leqslant 0.64$ ML on MgO{100} surfaces at $T = 5$ K show quantum excitations [10, 4]. Like in the case of isolated molecules [4], the spectra are characteristic of coupled reverse rotation of the molecule and its centre of mass according to the rotation–translation-coupling model [9]. This means that the protons of ammonia molecules do not localize orientationally as long as they undergo tunnelling. At the lowest coverages $\theta \leqslant 0.1$ ML the interaction with the surface determines the strength of the potential. At higher coverages this potential further increases due to increasing intermolecular interaction. The eccentricity of the centre-of-mass motion remains almost constant. Regimes of coverage-independent tunnelling energies and intensities increasing or decreasing linearly with θ are interpreted as the fingerprint of coexisting commensurate phases, which are identified. If the intermolecular distances become lower than 4.2 Å in the denser phases, intermolecular interaction reduces tunnelling to below the resolution of the instruments used (40 μeV), probably due to orientational ordering.

Ammonia molecules in the pure material [19] and physisorbed into MgO [11] reduce their dipolar energy by avoiding parallel orientations. This orientational structure is in contradiction to the form of the Hamiltonian used in the rotation–translation-coupling model. Thus for future data analysis, a modified RTC model based on a coupled rotation and nutation should be explored. For most materials where chemical bonds restrict molecular motion to a sphere, this represents a more realistic dynamics.

To support the outlined model, a diffraction experiment is planned to show the crystal structures directly. Furthermore, an inelastic neutron scattering experiment with partially

deuterated molecules should manifest an isotope effect which is characteristically different from that of the SP model [7].

Acknowledgments

We thank J Cook of the ILL very much for help with the experiment. Getting everything working was a great challenge after the long shutdown of the ILL. The experience and support of H Lauter helped significantly when we were starting this project. Discussions with G Voll, M Kolarschik, P Schiebel and W Prandl contributed to our understanding of the system under study.

References

[1] Smalley M, Hüller A, Thomas R K and White J W 1981 *Mol. Phys.* **44** 533
[2] Allen M P, Hovenden C B, Humes R P, Mehta S K, Thomas R K and White M A 1985 *Faraday Discuss. Chem. Soc.* **80** 171
[3] Larese J Z, Hastings J M, Passell L, Smith D and Richter D 1991 *J. Chem. Phys.* **97** 6997
[4] Havighorst M, Prager M and Coddens G 1996 *Chem. Phys. Lett.* **259** 1
[5] Press W 1981 *Single Particle Rotations in Molecular Crystals (Springer Tracts in Modern Physics 81)* (Berlin: Springer)
[6] Prager M and Heidemann A 1996 *Chem. Rev.* submitted
[7] Havighorst M and Prager M 1996 *Chem. Phys. Lett.* **250** 232
[8] Kearley G J, Coddens G, Fillaux F, Tomkinson J and Wegener W 1993 *Chem. Phys.* **176** 279
[9] Schiebel P, Hoser A, Prandl W, Heger G, Paulus W and Schweiß P 1994 *J. Phys. C: Solid State Phys.* **6** 10 989
[10] Kolarschik M and Voll G 1996 *Physica* B **222** 1
[11] Langel W 1996 *Chem. Phys. Lett.* **259** 7
[12] Degenhardt D 1988 *Doktorarbeit* Universität Kiel
[13] Young D M and Crowell A D 1962 *Physical Adsorption of Gases* (London: Butterworths)
[14] Sawabe K, Morokuma K and Iwasawa Y 1994 *J. Chem. Phys.* **101** 7095
[15] Lakhlifi A and Girardet C 1991 *Surf. Sci.* **241** 400
[16] Pugh S and Gillan M J 1994 *Surf. Sci.* **320** 331
[17] Ferro Y, Allouche A, Cora F, Pisani C and Girardet C 1995 *Surf. Sci.* **325** 139
[18] Echterhoff R and Knözinger E 1990 *Surf. Sci.* **230** 237
[19] Hewat A W and Riekel C 1979 *Acta Crystallogr.* A **35** 569
[20] Fillaux F and Carlile C J 1990 *Phys. Rev.* B **42** 5990
[21] Carlile C, McJamie I, Lockhart G and White J W 1992 *Mol. Phys.* **76** 173